ISSN 1674-1056
http://cpb.iphy.ac.cn
http://iopscience.iop.org/cpb
中国物理 B
Chinese Physics
中国物理
Chinese Physics B

Phase order in one-dimensional piecewise linear discontinuous map

Ru-Hai Du(杜如海), Sheng-Jun Wang(王圣军), Tao Jin(金涛), Shi-Xian Qu(屈世显)

Citation: Chin. Phys. B . 2018, 27(10): 100502. **doi:** 10.1088/1674-1056/27/10/100502

Journal homepage: http://cpb.iphy.ac.cn; http://iopscience.iop.org/cpb

What follows is a list of articles you may be interested in

Dynamic characteristics in an external-cavity multi-quantum-well laser

Sen-Lin Yan(颜森林)

Chin. Phys. B . 2018, 27(6): 060501. **doi:** 10.1088/1674-1056/27/6/060501

A new four-dimensional chaotic system with first Lyapunov exponent of about 22, hyperbolic curve and circular paraboloid types of equilibria and its switching synchronization by an adaptive global integral sliding mode control

Jay Prakash Singh, Binoy Krishna Roy, Zhouchao Wei(魏周超)

Chin. Phys. B . 2018, 27(4): 040503. **doi:** 10.1088/1674-1056/27/4/040503

Image encryption technique based on new two-dimensional fractional-order discrete chaotic map and Menezes-Vanstone elliptic curve cryptosystem

Zeyu Liu(刘泽宇), Tiecheng Xia(夏铁成), Jinbo Wang(王金波)

Chin. Phys. B . 2018, 27(3): 030502. **doi:** 10.1088/1674-1056/27/3/030502

Parameter analysis of chaotic superlattice true random number source

Yan-Fei Liu(刘延飞), Dong-Dong Yang(杨东东), Hao Zheng(郑浩), Li-Xin Wang(汪立新)

Chin. Phys. B . 2017, 26(12): 120502. **doi:** 10.1088/1674-1056/26/12/120502

A hybrid strategy to control uncertain nonlinear chaotic system

Yongbo Sui(隋永波), Yigang He(何怡刚), Wenxin Yu(于文新), Yan Li(李燕)

Chin. Phys. B . 2017, 26(10): 100503. **doi:** 10.1088/1674-1056/26/10/100503

Phase order in one-dimensional piecewise linear discontinuous map*

Ru-Hai Du(杜如海)[1,2], Sheng-Jun Wang(王圣军)[1,2], Tao Jin(金涛)[1,2], and Shi-Xian Qu(屈世显)[1,2,†]

[1] *Institute of Theoretical & Computational Physics, Shaanxi Normal University, Xi'an* 710119, *China*
[2] *School of Physics and Information Technology, Shaanxi Normal University, Xi'an* 710119, *China*

(Received 2 May 2018; revised manuscript received 17 July 2018; published online 10 September 2018)

The phase order in a one-dimensional (1D) piecewise linear discontinuous map is investigated. The striking feature is that the phase order may be ordered or disordered in multi-band chaotic regimes, in contrast to the ordered phase in continuous systems. We carried out an analysis to illuminate the underlying mechanism for the emergence of the disordered phase in multi-band chaotic regimes, and proved that the phase order is sensitive to the density distribution of the trajectories of the attractors. The scaling behavior of the net direction phase at a transition point is observed. The analytical proof of this scaling relation is obtained. Both the numerical and analytical results show that the exponent is 1, which is controlled by the feature of the map independent on whether the system is continuous or discontinuous. It extends the universality of the scaling behavior to systems with discontinuity. The result in this work is important to understanding the property of chaotic motion in discontinuous systems.

Keywords: chaos, piecewise discontinuous map, direction phase

PACS: 05.45.Pq **DOI:** 10.1088/1674-1056/27/10/100502

1. Introduction

Chaotic motion is a common phenomenon in many natural systems.[1–3] The well-known essential property of chaotic motion is highly sensitive to the initial condition. During the past few decades, the characteristics of chaos had been studied, and a variety of theoretical tools and methods were proposed and developed.[4–10] In a coarse-grained description, the direction phase introduced by Wang, Liu, and Hu translates the real coordinate of the trajectory into a binary symbolic encoding, and the net direction phase is defined to characterize the complexity of discrete chaotic systems.[5] The phase order has been widely studied in single maps, coupled systems, and also applied in data analysis. In a single discrete map, the system in a chaotic regime may show regular dynamical behavior in terms of phase order, i.e., the arrangement of the direction phase is ordered, and meanwhile it has been proved that the scaling behavior of the net direction phase at the transition point is an intrinsic feature of the map itself.[5,11] In analyzing practical data, the direction phase can expose the phase locking relationship between different time series.[12,13] In coupled chaotic systems, the direction phase has been widely used to characterize phase synchronization.[14–19]

However, most of the related researches mainly focus on systems that are continuous everywhere, so less work has been done for discontinuous systems.[15] Indeed, many realistic systems in different fields have the discontinuous property, such as electronic circuits,[20–23] relaxation oscillators,[24–26] and economic systems.[27] A typical representation of such systems is the piecewise linear map with a gap, and many interesting dynamic phenomena have been reported. Recently, there has been increasing interest in studying the new dynamical characteristics of discontinuous systems that are significantly different from those in the continuous systems.[28–30] In the view of cyclicity of chaotic attractors, it was found that multi-band chaotic attractors in continuous maps are cyclic, while those in maps with discontinuities may be acyclic.[29] We have to emphasize that the dynamical properties of discontinuous systems are far from being understood.

In this paper, we study the phase order in a one-dimensional (1D) discontinuous map, which is used to represent the normal form of piecewise linear discontinuous systems. We present that the phase order in a multi-band chaotic regime may be ordered or disordered, while it is ordered in continuous systems. The mechanism of this phenomenon roots in the relative position of the unstable fixed point to the re-injecting segment of the map. Moreover, the change of phase order is sensitive to the complex bifurcation structure of dynamics. In addition, the scaling exponent of the net direction phase at a certain transition point is determined by the feature of the mapping function, which agrees with that in continuous systems.[11] These results may help us to get deep insight into the essence of discontinuous systems.

2. Model and method

The model employed in this work is a 1D piecewise linear discontinuous map, which usually describes an ideal switch-

*Project supported by the National Natural Science Foundation of China (Grant No. 11645005) and the Interdisciplinary Incubation Project of Shaanxi Normal University (Grant No. 5).

†Corresponding author. E-mail: sxqu@snnu.edu.cn

© 2018 Chinese Physical Society and IOP Publishing Ltd

ing in electronic switching circuits. Its bifurcation analysis has been reported in many researches.[21–23] The map has a general form

$$x_{n+1} = \begin{cases} f_{\rm L}(x_n) = ax_n + \mu, & \text{if } x_n \le 0, \\ f_{\rm R}(x_n) = bx_n + \mu + l, & \text{if } x_n > 0, \end{cases} \tag{1}$$

where a, b, μ, and l are parameters. There is a discontinuous boundary at $x = 0$ where the left and right limits of the mapping function are not identical. The symbols $f_{\rm L}$ and $f_{\rm R}$ stand for the left and right branch of the mapping function, respectively. The two critical values are $f_{\rm L}(0) = \mu$ and $f_{\rm R}(0) = \mu + l$. In this work, we set parameters $a = -0.6$, $b = -1.4$, $l = 0.8$, and μ as a varying control parameter. According to the linear stability analysis, the system has two fixed points, i.e., a stable fixed point $x^*_{\rm L} = \mu/(1-a)$ in $f_{\rm L}$, and an unstable fixed point $x^*_{\rm R} = (\mu + l)/(1-b)$ in $f_{\rm R}$. When $\mu < 0$, all orbits converge to $x^*_{\rm L}$. When $\mu > 0$, there is only one unstable fixed point $x^*_{\rm R}$.

Figures 1(a) and 1(b) show the bifurcation diagram and the Lyapunov exponent as μ varies. The chaotic attractors exist in the region (μ_0, μ_3) between the two periodic regimes and show a complex bifurcation structure. When $\mu_0 < \mu < \mu_1$, the chaotic attractors show the multi-band structure. At μ_1 two chaotic bands merge into one band. The critical point $\mu_1 = 0.1716$ is obtained by the collision between the attractor boundary and the unstable fixed point $x^*_{\rm R}$. As μ goes to μ_2, the single band decomposes into two chaotic bands, and then multiple bands as it increases afterward. This crisis is due to the collision between the critical value $f_{\rm L}(0)$ and the unstable fixed point $x^*_{\rm R}$, which give the critical point $\mu_2 = -l/b = 0.5714$.

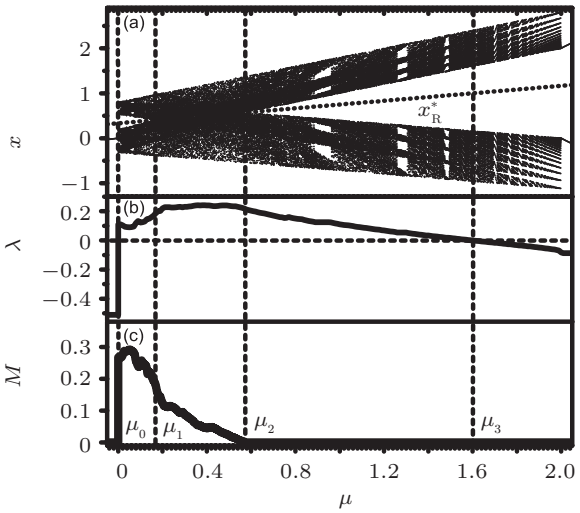


Fig. 1. Bifurcation diagram, Lyapunov exponent, and the net direction phase, plotted in panels (a), (b), and (c), respectively. The vertical dotted lines denote the bifurcation points μ_0, μ_1, μ_2, and μ_3.

For a discrete map, the direction phase is defined as follows. If $x_{n+1} > x_n$, we get an up phase denoted by $S(n) = 1$, and when $x_{n+1} < x_n$, we get a down phase denoted by $S(n) = -1$. A special example is the period-1 orbit, i.e., $x_{n+1} = x_n$, the phase index is $S(n) = 0$. In order to investigate the regularity of the chaotic attractors, we examine the net direction phase as μ varies. The net direction phase M is calculated from the time average of $S(n)$ over a long enough trajectory,

$$M = \frac{1}{T}\sum_{n=1}^{T} S(n). \tag{2}$$

$M = 0$ means that the phase order is regular. Otherwise, $M \neq 0$, which indicates a disordered phase.

3. Results and discussion

Previous work on continuous maps shows that the phase order always exhibits regular arrangement in the multi-band chaotic regime, while at the band merging point the regular arrangement becomes irregular. However, in this work, we find that the phase order presents a different picture. The dependence of the net direction phase M on the control parameter μ is shown in Fig. 1(c). In the calculation of M, we start from initial value $f_{\rm R}(0)$ to make sure the trajectory is always inside the attractors, and 10^5 iterations are recorded for the time average at each parameter value. A trivial result appears when the system is in the periodic regime, where $M = 0$. In the region $\mu_2 < \mu < \mu_3$, the system shows a multi-band structure and we obtain a regular phase order because $M = 0$. As μ is decreased, a transition of the net direction phase from zero to positive value arises at the bifurcation point μ_2. After that, we obtain the disordered phase, which lasts till μ_0. It should be noted that at the bifurcation point μ_1, the two chaotic bands merge into one single band, but the transition of phase order does not occur. Obviously, the phase order behaviors of the chaotic attractors in the two regions are significantly different, which presents an example for the rich transition scenarios due to the discontinuous feature of the current system.

The complex transitions on the phase order described above are governed by the characteristic of the mapping function as shown in Fig. 2. One may see that any trajectory through the left branch may move to the right branch after one iteration, which gives rise to a positive phase order $S(0) = 1$. It then iterates cyclically around the unstable fixed point $x^*_{\rm R}$ for some time n before it re-injects into the left branch, by which the trajectory makes a round trip. Where, the n-th iteration contributes a negative phase order $S(n) = -1$. The sum of the phase orders in this round trip depends on the parity of n. When n is even, we have the same number of up and down phases, and thus the sum of the phase orders of the iterations on the right branch is 0. So the sum in the round trip is 1. On the contrary, if n is odd, the first $n-1$ iterations make pairs and the phase order $S(n) = -1$ canceled out the initial phase order $S(0) = 1$. Thus, the sum in this round trip is zero.

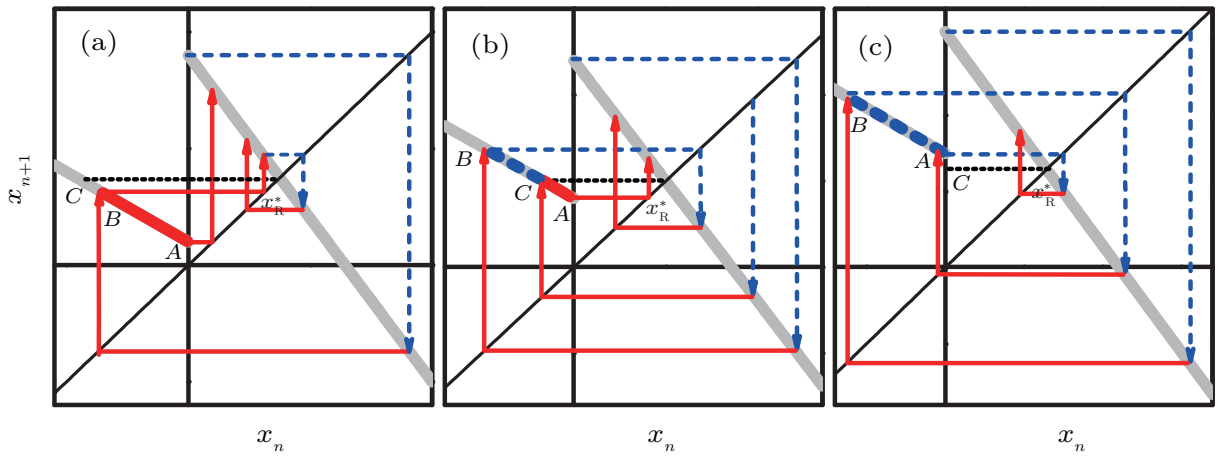


Fig. 2. (color online) Mapping functions for three different parameters: (a) $\mu = 0.1$, (b) $\mu = 0.4$, and (c) $\mu = 0.7$. The red (blue) lines indicate the points in f_L map onto f_R with up (down) phase.

Obviously, the overall net phase order is governed by the details of the map. To explain how the map function influences the net phase order, drawn in Fig. 2 are the mapping functions at three typical control parameters. There are three important points A, B, and C in each of the plots, where A denotes the local minimum of the mapping function, B denotes the local maximum whose horizontal coordinate is itself the bottom border of the attractor, and C is the intersection of the mapping function with the horizontal line connecting the fixed point x_R^*. The former case occurs in Fig. 2(a), where point C is on the left side of point B and thus the vertical coordinate of any point in segment AB is lower than x_R^*. Therefore, in any round trip of the iteration process starting from (re-injecting at) segment AB, the iteration in the right side produces an equal number of up and down phases from any of the points in segment AB. Suppose there are L rejections, and n_i iterations in the i-th round trip, then the net phase order reads (according to the definition in Eq. (2)),

$$M = \frac{L}{\sum_{i=1}^{L} n_i}. \tag{3}$$

While the latter case occurs when the control parameter $\mu \geqslant \mu_2$ as shown in Fig. 2(c), where point C is on the right side of A. In any round triple starting from anywhere in segment AB, the number of iterations in the right side is odd. Thus the net phase is $M = 0$. When $\mu_1 \leqslant \mu < \mu_2$, things becomes a bit complicated, where point C enters segment AB and divides it into two pieces, i.e., BC and CA. The re-injecting points may fall in either BC or CA. If it is in CA, the net phase order is calculated by Eq. (3). If it is in BC, the net phase order is zero. Generally, we have

$$M = \frac{\sum_{i=1}^{L} n_i \bmod 2}{\sum_{i=1}^{L} n_i}. \tag{4}$$

Actually, the summation in the numerator of Eq. (4) is the number of round trips with an even number of iterations in the right branch (i.e., $n_i - 1$ is even), denoted by N_e. The denominator is the total number of iterations, i.e., T. Thus, the net phase can be defined by the ratio $M = N_e/T$. To test this relevance, we start an iteration process that persists for $T = 10^4$ time steps at given $\mu \in (0, \mu_2)$, and then plot in Fig. 3(a) all the trajectories in the round trips through segment CA and record the number of this type of round trips and denote it by N_e. Where the blue line marked by B is the horizontal coordinate of point B, i.e., $x_B(\mu)$, the red line marked by C is the horizontal coordinate of C, i.e., $x_C(\mu)$, and the intersect of these two lines gives the value of the critical parameter μ_1. The control parameter dependence of the ratio $R = N_e/T$ is shown in Fig. 3(b), which agrees very well with the result in Fig. 1(c).

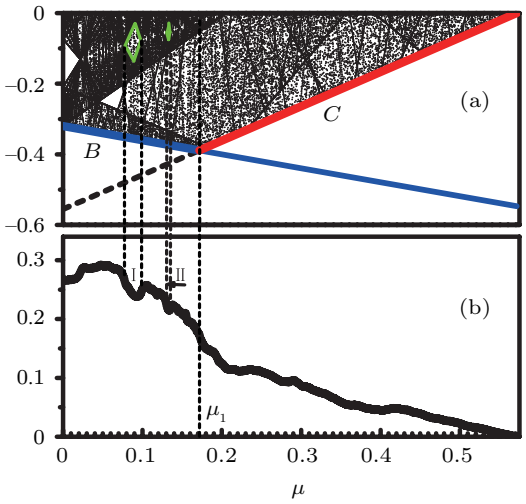


Fig. 3. (color online) The density distribution of the orbital points in CA (a) and the ratio R (b).

Considering the definition of the ratio R (or net phase order M), figures 3(a) and 3(b) tell the same thing. Figure 3(a) is only a visualized representation of Fig. 3(b), in which the gray scale actually shows the density of trajectories visiting the interval $[x_B(\mu), 0]$ in phase space. In the figure, one may

see that there are a great many dark lines, which are the forward images of the discontinuous boundary in the mapping function. The intersection of those dark lines produces a great many cross points, and also confines many forbidden regions in some situations. Meanwhile, the band merging occurs as soon as the cross points that confine the forbidden regions inside the attractor collide with an unstable orbit. Those processes have a deep influence on the density distribution and the net phase order.

When $\mu \leqslant \mu_1$, the net phase or ratio R is determined by the magnitude of n_i and the size of attractor for a given iteration sequence of length T according to Eq. (4). The darker the point in Fig. 3(a) is, the smaller n_i is. In the range where $\mu \in [0, 0.0220]$, the attractor is a five-band chaotic attractor, as shown by the very dark area of the figure. Thus we have a relatively bigger R value. It increases as μ increases since the size of the attractor increases and meanwhile the decreasing on the size of the forbidden region also induces additional increasing of the attractor size. Near $\mu \simeq 0.0220$, it has an obvious uplift, which is due to the bands merging of the attractor. When $\mu \in [0.0220, 0.0765]$, the variation of R is flat since the increasing on the sizes of the attractor and the forbidden region happen simultaneously. After that, we uncover an interesting phenomenon, i.e., R undergoes a rapid decreasing firstly and then a very fast increasing, as shown in the special intervals marked by I and II in the figure. The lozenge regions surrounded by the green lines in Fig. 3(a) are a response to this special variation. They are sparsely filled by the trajectories. The broadening of those regions inside segment AB definitely results in the decreasing of R because the low density means the large n_i in a round trip of iterations for a given T. Therefore, the special shape of those sparse regions implies the opposite tendency of R against the variation of the shape itself. Those phenomena can be frequently encountered considering the self-similar structure of the chaotic attractor and the bifurcation process. Apparently, things may become simpler despite the change of the forbidden regions and the sparse regions, and the merging of chaotic bands happens very often when $\mu > \mu_1$. The reason is that only the round trip of iterations whose trajectories visit segment CA contribute a nonzero net phase order to R, and the length of CA decreases as μ is increasing. Therefore, we found a decent tendency of R in Fig. 3(b). When $\mu \geqslant \mu_2$, the length of CA goes to zero and thus $R = 0$.

In addition, we also observed the scaling behavior of the net phase order as μ is very close to the critical point μ_2, where the band merging appears. The result is shown in Fig. 4. In the continuous maps, the reported work reveals that the scaling exponent is inversely proportional to the exponent of the mapping function.[5,11] Here, in this discontinuous map, the mapping function is linear. The fitted slope of the line in the double logarithm plot in the figure is 1.013 ± 0.003, and the intercept is -1.12 ± 0.02. It supports the conclusion in the continuous map. According to the density distribution in Fig. 3(a), we may get an analytical proof of the scaling by roughly assuming that the trajectories of the chaotic attractors visit segment AB with a uniform probability density. It is to say that the net phase order can approximately equal to the ratio of the length CA over AB, i.e., $M(\mu) = |x_C(\mu)|/|x_B(\mu)|$. Simple calculation yields

$$\ln M = \ln \delta + \ln \frac{b^2}{a(1+b)(1-b)^2 l}. \tag{5}$$

where $\delta = \mu_2 - \mu$. The scaling exponent is exactly 1, which agrees very well with the numerical result, while the analytical value of the intercept is 0.572, which is greater than the numerical one. The reason is that there are actually many forbidden regions in segment CA where the trajectory cannot enter. In this rough estimation, it over counts this area into the nonzero net phase; however, the physics revealed by Eq. (5) is right.

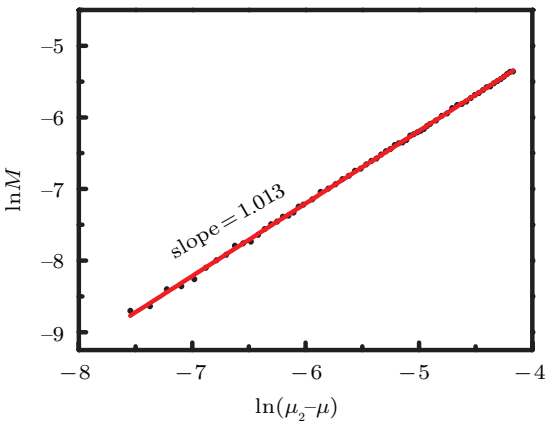


Fig. 4. (color online) The scaling of M near the critical point μ_2.

4. Conclusion

In this paper we investigate the phase order in a 1D piecewise linear discontinuous map. We have uncovered that the regularity of phase order for the continuous map is not applicable for the discontinuous map. The phase order in the multi-band chaotic regimes may be ordered or disordered, in contrast to those in continuous systems where only the order phase dominates. Our analysis reveals that the key to affecting the transition of the phase order is the relative position the unstable fixed point with respect to the re-injection segment AB. Numerical computation displays that the direction phase is sensitive to the density distribution of trajectories of the attractors. The scaling behavior of the net direction phase at a transition point is also observed, and the analytical expression of it is obtained. The scaling exponent is determined by the feature of the map involved in the problem, which has no

intrinsic difference against the continuous counterpart. It extends the universality of scaling behavior to the system with discontinuity. The complex behaviors of the net phase in the current work reveal rich dynamical phenomena in discontinuous systems.

References

[1] Ott E 2006 *Chaos in Dynamical Systems* (Beijing: Beijing World Publishing Corporation)
[2] Fečkan M 2011 *Bifurcation and Chaos in Discontinuous and Continuous Systems* (Bejing: Higher Education Press)
[3] Strogatz S H 2015 *Nonlinear Dynamics and Chaos: With Applications to Physics, Biology, Chemistry, and Engineering* (Westview Press)
[4] Grebogi C, Ott E and Yorke J A 1982 *Phys. Rev. Lett.* **48** 1507
[5] Wang W, Liu Z H and Hu B B 2000 *Phys. Rev. Lett.* **84** 2610
[6] Wang X and Chen G R 2013 *Nonlinear Dyn.* **71** 429
[7] Dudkowski D, Jafari S, Kapitaniak T, Kuznetsov N V, Leonov G A and Prasad A 2016 *Phys. Rep.* **637** 1
[8] Han Q, Liu C X, Sun L and Zhu D R 2013 *Chin. Phys. B* **22** 020502
[9] Yang K L, Chen H Y, Du W W, Jin T and Qu S X 2014 *Chin. Phys. B* **23** 070508
[10] Lei Y M and Zhang H X 2017 *Chin. Phys. B* **26** 30502
[11] Shrimali M D and Ramaswamy R 2002 *Phys. Lett. A* **295** 273
[12] Park K, Lai Y C, Liu Z H and Nachman A 2004 *Phys. Lett. A* **326** 391
[13] Liu Z H, Hu B B and Iasemidis L D 2005 *Europhys. Lett.* **71** 200
[14] Jalan S and Amritkar R E 2003 *Phys. Rev. Lett.* **90** 014101
[15] Tucci K, Cosenza M G and Llamoza O A 2003 *Phys. Rev. E* **68** 027202
[16] Zhou Y Z, Zhou J and Liu Z H 2008 *Europhys. Lett.* **84** 60001
[17] Zhou Y Z, Zhou J, Wang X G, Guan S G, Lai C H and Liu Z H 2010 *Europhys. Lett.* **90** 30005
[18] Liang X M, Lü H P and Liu Z H 2008 *Chin. Phys. Lett.* **25** 409
[19] Yang Y J, Du R H, Wang S J, Jin T and Qu S X 2015 *Chin. Phys. Lett.* **32** 010502
[20] Asahara H, Izumi Y, Tone Y, Matsumoto H and Kousaka T 2014 *Circ. Syst. Signal. Pr.* **33** 2695
[21] Jain P and Banerjee S 2003 *Int. J. Bifur. Chaos* **13** 3341
[22] Avrutin V, Schanz M and Banerjee S 2006 *Nonlinearity* **19** 1875
[23] Avrutin V, Gardini L, Schanz M and Sushko I 2014 *Int. J. Bifur. Chaos* **24** 1440012
[24] He D R, Wang B H, Bauer M, Habip S, Krueger U, Martienssen W and Christiansen B 1994 *Physica D* **79** 335
[25] Qu S X, Wu S W and He D R 1998 *Phys. Rev. E* **57** 402
[26] Qu S X, Lu Y Z, Zhang L and He D R 2008 *Chin. Phys. B* **17** 4418
[27] Gardini L, Sushko I and Naimzada A K 2008 *J. Econ. Theor.* **143** 541
[28] Colombo A, Bernardo M D, Hogan S J and Jeffrey M R 2012 *Physica D* **241** 1845
[29] Avrutin V, Sushko I and Gardini L 2013 *Math. Comput. Simul.* **95** 126
[30] Castro J, Alvarez J, Verduzco F and Palomares-Ruiz J E 2017 *Chaos, Solitons, and Fractals* **105** 8